# Conformational Study in Water by NMR and Molecular Modeling of α-Methyl-α-Amino Acid: Differential Conformational Properties of α-Cyclic and α-Methylglutamic Acid

Nathalie Todeschi,[†] Josyane Gharbi-Benarous,[†,‡] Veerappan Arulmozhi,[†] Francine Acher,[†] Robert Azerad,[†] and Jean-Pierre Girault*[,†]

Laboratoire de Chimie et Biochimie Pharmacologiques et Toxicologiques (URA 400 CNRS), Université René Descartes, 45 rue des Saint-Pères, 75270 Paris Cedex 06, France, and UFR Chimie, Université Paris 7, Denis Diderot, 2 Place Jussieu, F-75251 Paris Cedex 05, France

Received August 20, 1996[⊗]

The 2-methylglutamic acid (**2M**) analogue was generally inactive in electrophysiological experiments and had generally worse functional activity. The low functional activity obtained with **2M** would not be determined by only α substitution or C methylation, since the extensive biological studies of α,α′-dialkyl cyclic analogues of glutamic acid containing a cyclohexane and a cyclopentane ring or $\beta$- or $\gamma$-methylated glutamic acid analogues with linear flexible systems have indicated interesting properties. A conformational analysis by $^{1}$H and $^{13}$C NMR spectroscopy and molecular modeling of **2M** was undertaken in aqueous solution to identify the preferred solution conformations and to understand whether its different biological activities would be due to structural differences. The preferred conformation of the **2M** molecule is the sterically favored one Ca, corresponding to a large "W" between the methyl and the carboxylate groups mixed with Aa showing a large zig−zag alkylamine chain ending in a carboxylate group, or Ba, corresponding to a large "W" between the amino and the carboxylate groups.

## INTRODUCTION

Considerable recent interest has been generated in the pharmacology of acidic amino acids related to glutamic acid because of the perceived role of these compounds in various biological functions as synaptic transmitters in the mammalian central nervous system,[1,2] as substrates or inhibitors of the D-glutamate-adding enzyme from *Escherichia coli*[3] and, previously, as substrates of glutamine synthetase.[4]

Glutamate is responsible for the fast excitatory synaptic transmission[1,5] and plays important roles in synaptic plasticity phenomena involved in brain development, learning, and memory.[6] Glutamate is also the main endogenous neurotoxin, being responsible for neuronal death observed after ischemia, hypoxia, or hypoglycemia.[7] Glutamate is therefore assumed to be involved in neurological disorders such as Parkinson's and Alzheimer's diseases and Huntington's chorea.[8] Glutamate activates two types of receptors, the ionotropic and the metabotropic.[9,10] The ionotropic receptors are classified into two main categories, those for which the synthetic glutamate analogue *N*-methyl-D-aspartic acid is a potent excitant (NMDA receptors) and those on which NMDA is not active (non-NMDA) [(α-aminohydroxy)-5-methyl-4-isoxazolepropionate (AMPA) or kainic acid (KA)],[5] and, in addition to these ionotropic receptors, the metabotropic L-Glu receptors.[11,12] Recently, molecular cloning studies have revealed a family of metabotropic receptors termed mGluR1 to mGluR8.[10,13] Interestingly, these receptors are involved in glutamate-induced synaptic plasticity and in spacial and olfactory memory.[14]

One of the choice methods, to analyze the diversity of the receptors that mediate the neuronal events, is to produce rigid analogues of glutamic acid:

(i) First, the introduction of conformationally restricted cyclic analogues of natural amino acids in substrates or inhibitors has already proved helpful for studies of the geometry of binding sites.[15,16] The isomeric glutamic acid analogues containing a cyclohexane ring, the *cis*- and *trans*-1-aminocyclohexane-1,3-dicarboxylic, the *cis*- and *trans*-C6 (Figure 1a) or a cyclopentane ring, the *cis*- and *trans*-1-aminocyclopentane-1,3-dicarboxylic acid (ACPD), the *cis*- and *trans*-C5 (Figure 1a), have already been tested for some biological properties in comparison to glutamic acid. Among the two isomers, only the *cis*-C6 derivative is ∼10 times more potent than the trans isomer as an agonist of the ionotropic KA receptor of the central nervous system.[17] The *cis*-C5 (*cis*-ACPD) isomer is an agonist of NMDA receptor[15] while the *trans*-C5 (*trans*-ACPD) isomer is a specific agonist of metabotropic glutamate receptors (ACPD receptor).[18]

These derivatives, such as cyclic analogues of glutamic acid containing a cyclohexane and a cyclopentane ring (Figure 1a), have already been submitted to conformational analysis in an aqueous environment by NMR spectroscopy and molecular dynamics (MD).[19,20]

(ii) Also, the methylation effect at $\beta$ or $\gamma$ leads to barrier heights of the order of 3−12 kcal mol$^{-1}$ according to the $\beta$- or $\gamma$-methylated glutamic acid analogues, which may hinder the interconversion between the rotamers relative to a single bond. We have studied the conformation of the linear methylated analogues.[21] In these molecules, there is a some degree of liberty around the C(2)−C(3) torsion angle $\chi$1 and the C(3)−C(4) torsion angle $\chi$2 (Figure 1b). Biological studies of the compounds capable of modulating the glutamate receptor function of central nervous system have demonstrated that the (*R*)-4-methylglutamic acid isomer has exceptional selectivity for the ionotropic KA receptor with an $IC_{50}$ for inhibition of KA binding comparable to kainic acid itself[22] while the ligand (*S*)-4-methylglutamic acid interacts especially at the metabotropic glutamate receptor mGluR1a

[†] Université René Decartes.
[‡] Université Paris 7.
[⊗] Abstract published in *Advance ACS Abstracts,* February 15, 1997.

S0095-2338(96)00052-2 CCC: $14.00 

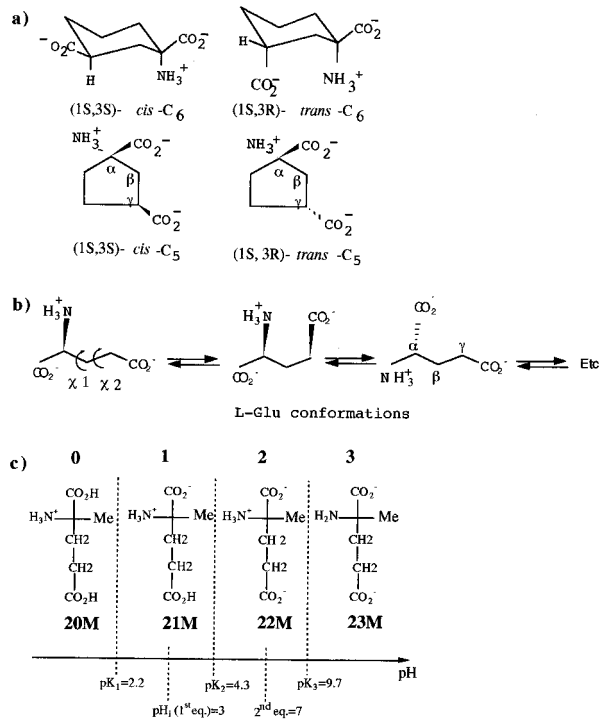


**Figure 1.** (a) Structures of *cis*-C6, *trans*-C6 and *cis*-C5, *trans*-C5 analogues of glutamic acid in aqueous solution at pH 7 (isomers α-*S* represented). (The definition of cis and trans is relative to the arrangement of the carboxyl function. *cis*-C6 or -C5 is an equimolecular mixture of 1*S*,3*S* and 1*R*,3*R* and *trans*-C6 or -C5 an equimolecular mixture of 1*S*,3*R* and 1*R*,3*S*); (b) conformations of L-glutamic acid around neutral pH; (c) predominant forms of **2M** isomer in the different pH zones (from 0 to 3).

with an $EC_{50}$ comparable to glutamic acid itself.[23]

The 2-methylglutamate (substituted at the same carbon as C6 and C5 derivatives) was tested in electrophysiological experiments,[23] and its action on ionotropic (NMDA and AMPA) and metabotropic receptors was studied. The effect of the compound on depolarizations induced by (1*S*,3*R*)-ACPD and L-glutamate, and also on L-AP4-induced depressions of evoked mono- and polysynaptic responses were also examined. The 2-methylglutamic acid analogue was generally inactive in all studies, even when tested up to 2 mM. However, at much lower doses it potentiated L-AP4-induced depressions of monosynaptic activity, exerted modulatory effect at presynaptic metabotropic glutamate receptors of the L-AP4 type, but had no marked agonist activity itself at other presynaptic mGluR's. This compound was previously tested on mGluR1a receptors expressed in *Xenopus oocytes* and has been identified as having worse activity for this receptor (with an $EC_{50}$ of 600 μM; not comparable to glutamic acid itself, $EC_{50}$ of 10 μM).

This compound has generally worse functional activity, though ring closure imposes conformational constraints and limitations not existing in this linear flexible molecule (Figure 1b). But, one of the chemical tools potentially available for structure stabilization in peptides is the incorporation of α-methylated α-amino acids,[24] because of severe restrictions of the rotational freedom around the N−C(α) and C(α)−CO bonds.[25]

Since the extensive biological studies of α,α′-dialkyl cyclic analogues, the low functional activity obtained with 2-methylglutamic acid (**2M**) would not be determined only by α-substitution or by C-methylation. Indeed, the biological studies of β- or γ-methylated glutamic acid analogues with linear flexible systems have indicated interesting properties. The latter derivatives are substituted in position β or 3 and γ or 4 by a methyl group; thus the structural changes in **2M** would not be expected to induce many conformational differences but apparently they profoundly affect its biological properties.

Also, the conformational analysis study of this α-substituted amino acid is very important since it provides good information about the induction of helical structure.[26,27] The stabilization of particular conformational properties has been of major interest in the field of biologically active peptides, and more recently, the induction or stabilization of secondary structures in peptides by α-methylated amino acids has also become a major issue in conjunction with the de novo design of proteins.

## RESULTS AND DISCUSSION

**Conformational Analysis.** A NMR and MD study in aqueous solution at pH 7 (**22M**) of **2M** (Figure 1c) will be developed here, in order to explore fully the conformational space of this compound. The protonation site would induce particular conformations; thus, the NMR and MD studies include an extensive conformational analysis in water at different pH values: (i) the case of **21M**, the γ-carboxylate group bearing a proton (isoelectric pH 3, zwitterionic form) that can provide a γ-carboxylic group (γ-$CO_2H$) which possesses a potential proton donor hydroxyl group; (ii) the case of **23M**, the amino group carrying no formal charge (pH 11). Hence it was interesting to examine the conformational change induced by the electrostatic field generated by the different polarities of these molecules.

Computational investigation was undertaken in water in order to elucidate the conformational characteristics in a biological-type environment and then provide information on the dynamic behavior of the different isomers as well as on their hydration. The aim of the conformational analysis is to find all the thermally populated conformations of a molecule, i.e., the conformations with the lowest free energies, in order to provide important structural information on the properties of the molecule. The methodology presented illustrates the usefulness of MD in elucidating possible solution conformations and of NMR data in revealing that approximate solution structures can be estimated.

The final structures obtained after several molecular modeling calculations were examined for overall energetic favorability and compared with the structure derived from the NMR data. The torsion angles of generated structures can be correlated to the corresponding coupling constants by using Karplus-type equations.[28−31] The structural information of the different conformations generated by MD is compared to the NMR parameters. Thus, NMR parameters reflect the virtual conformation, and at the same time, the structural information of the different conformations generated by MD is of great benefit in predicting the conformations in solution.

Discussing rotation about $sp^3-sp^3$ carbon−carbon bonds, two degrees of conformational freedom are apparent (Figure 1b), namely, rotation about the two C(2)−C(3) and C(3)−C(4) bonds; the corresponding torsion angles are labeled χ1 [α-$CO_2^-$−C(2)−C(3)−C(4)] and χ2 [$^+$NC(2)−C(3)−C(4)−γ$CO_2^-$]. Figure 2a shows three staggered conformations.

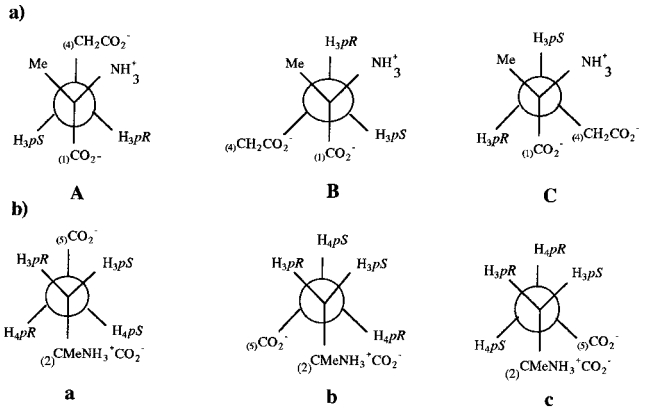


**Figure 2.** Newmann projections of the three "staggered" rotamers about the C2−C3 and C3−C4 bonds of the amino acid **2M** (a) **A**, **B**, and **C** relative to the torsion angle $\chi 1$ (viewed in the C2 → C3 direction); (b) **a**, **b**, and **c** relative to the $\chi 2$ one (viewed in the C3→C4 direction).

**Table 1.** $^1$H and $^{13}$C Chemical Shifts in $D_2O$ at Various pH Values ($\delta$/[$^2H_4$]TSP) (H Denoted a or b According to the Stereospecificity of the Proton)

| | **2M**[a] | | | | | |
|---|---|---|---|---|---|---|
| | **21M**[b] pH 3 | **21M**[c] pH 3 | **22M**[b] pH 7 | **22M**[c] pH 7 | **23M**[b] pH 11 | **23M**[c] pH 11 |
| 1 | | 178.5 | | 179.6 | | 185.8 |
| 2 | | 62.8 | | 63.9 | | 61.3 |
| 2Me | 1.56 | 24.9 | 1.50 | 25.3 | 1.27 | 28.1 |
| 3a | 2.19 | 35.2 | 2.08 | 36.3 | 1.92 | 40.1 |
| 3b | 2.16 | | 2.03 | | 1.77 | |
| 4a | 2.56 | 34.9 | 2.32 | 35.2 | 2.20 | 35.9 |
| 4b | 2.49 | | 2.25 | | 2.09 | |
| 5 | | 181.0 | | 184.2 | | 186.6 |

[a] The first number indicates the position of the methyl (at carbon **2**), the second one the predominant form in the pH zone considered (isoelectric zone **1**, neutral zone **2**, and alkaline zone **3**), the letter **M** denotes the methyl substituents. [b] $^1$H. [c] $^{13}$C.

**Table 2.** Homonuclear ($^1$H−$^1$H) and Heteronuclear ($^{13}$C−$^1$H) Coupling Constants in $D_2O$ Used in the Conformational Analysis of the **2M** Isomer and for the Assignment of the Diastereotopic Methylene Protons at C(3) and C(4)

| | **2M** | | |
|---|---|---|---|
| | **21M** pH 3 | **22M** pH 7 | **23M** pH 11 |
| | J/Hz | | |
| $^2J_{HH}$ | | | |
| 3a, 3b | −15.6 | −15.6 | −12.0 |
| 4a, 4b | −15.5 | −15.5 | −14.3 |
| $^3J_{HH}$ | | | |
| 3a, 4a | 9.3 | 10.0 | 11.6 |
| 3a, 4b | 7.4 | 6.5 | 4.8 |
| 3b, 4a | 7.0 | 5.7 | 5.0 |
| 3b, 4b | 9.2 | 10.3 | 12.1 |
| $^3J_{CH}$ | *a* | | *a* |
| 3a-H, 1-C | | 1.4 | |
| 3a-H, 2Me-C | | 2.6 | |
| 3a-H, 5-C | | <2 | |
| 3b-H, 1-C | | 5.2 | |
| 3b-H, 2Me-C | | 1.5 | |
| 3b-H, 5-C | | <2 | |
| 4a-H, 2-C | | 3.3 | |
| | Assignment | | |
| 3a-H | pro-*R* | pro-*R* | pro-*R* |
| 3b-H | pro-*S* | pro-*S* | pro-*S* |
| 4a-H | pro-*S* | pro-*S* | pro-*S* |
| 4b-H | pro-*R* | pro-*R* | pro-*R* |
| | populations of rotamers[b] about $\chi 1$ and $\chi 2$/% | | |
| **A** | *a* | 15 | *a* |
| **B** | | 15 | |
| **C** | | *70* | |
| *a* | *50* | *75* | *94* |
| **b** | 25 | 10 | 3 |
| **c** | 25 | 15 | 3 |

[a] Heteronuclear ($^{13}$C−$^1$H) coupling constants in acidic and basic solution are difficult to measure. Thus, it is not possible to evaluate the population of rotamers corresponding to the $\chi 1$ rotor, at alkaline and acidic pH values. [b] The major populations of rotamers about $\chi 1$ and $\chi 2$ are in italics.

These conformers are designated according to the trans orientation relative to each other of the backbone chain and one α-group: respectively, the α-carboxylate group (**A**), the α-amino group (**B**), and the α-methyl group (**C**). In the system C(3)−C(4) (Figure 2b), the torsion angle about C(3)−C(4) is defined according to the disposition of the γ-carboxylate group relative to the side chain, trans (*t*-**a**) or gauche ($g^+$-**b** and $g^-$-**c**). The conformers **b** and **c** seem of identical energy. In biomolecules, and even in relatively simple ones, the conformational problem is often quite complex. As a consequence, their conformational dynamics remains interesting to explore.

**First Part: NMR. (a) Assignments.** The proton and carbon assignments can be made from one-dimensional spectra recorded from AMX 500 spectrometer and are given in Table 1. Carbon assignments were deduced from the broad-band decoupled $^{13}$C spectrum, DEPT 135[32] experiment, and the $^{13}$C chemical shifts of the product in $D_2O$ solution were assigned almost completely. Those of the carboxylate groups (α- and γ-$CO_2^-$) and of the methylene groups (3-$CH_2$ and 4-$CH_2$) were more difficult since their chemical shifts are very close. In each case, one was expected to be $^1$H, $^{13}$C long-range coupled to 2-methyl. A selective INEPT experiment[32−34] was thus performed, and a selective $^1$H pulse on the 2-Me led to a selective polarization transfer to the signal at $\delta$ 179.5 ppm assigned to C(1) (α-$CO_2^-$) and to the signal at $\delta$ 36.3 ppm assigned to C(3) (3-CH2). In order to confirm the interpretation of chemical shifts of H(3a), H(3b), and H(4a), H(4b), an inverse heteronuclear correlation $^{13}$C−$^1$H COSY experiment was carried out.[35] Thus, it is possible to confirm the attribution of corresponding protons H(4a), H(4b) with higher frequency and H(3a), H(3b) with lower frequency as they are simultaneously coupled to the carbon at C(4) (35.2 ppm) and C(3) (36.3 ppm), respectively. The chemical shifts of the four different protons are evaluated without any ambiguity. From the temperature dependence, it can be seen that the values of chemical shifts do not change appreciably as we increase the temperature; this may be due to lesser interaction between solute and solvent molecules which leads to weaker hydrogen bonding. Me(2) and H(3) protons chemical shifts are less sensitive to the temperature than those of H(4), indicating a protection of these protons from the water solvent.

Qualitative considerations are often used for diastereotopic assignment of methylene protons (it is assumed that predominantly staggered rotamers are populated).[36] Accurate homo- and heteronuclear coupling constants can serve to determine the population of the rotamers (Figure 2). The attribution pro-*R* to H(3a) and pro-*S* to H(3b) is essentially obtained by analyzing all the coupling constants values $^3J_{HH}$ and $^3J_{CH}$ from H(3a) and H(3b) (See below). All the characteristic parameters are shown in Table 2.

**Table 3.** Torsion Angles (deg) and Calculated[a] Coupling Constants ($^3J$/Hz, in Parentheses) Computed for **2M**, from the Different Conformations Generated by MD at Neutral pH

| | **2M** | | | | | | | | |
|---|---|---|---|---|---|---|---|---|---|
| | Aa | Ab | Ac | Ba | Bb | Bc | Ca | Cb | Cc |
| 3*R*,4*S* | 172.5 | 60.4 | −55.6 | 173.9 | 76.9 | −65.4 | −173.3 | 50.1 | −73.5 |
| | (12.2) | (3.3) | (3.8) | (12.3) | (1.8) | (1.1) | (12.2) | (4.7) | (2.0) |
| 3*R*,4*R* | −70.2 | 173.9 | 57.2 | −68.7 | −168.7 | 47.9 | −56.2 | 162.8 | 40.8 |
| | (2.3) | (12.3) | (3.7) | (2.4) | (12.0) | (5.0) | (3.8) | (11.5) | (6.1) |
| 3*S*,4*R* | 177.1 | 63.0 | −52.7 | 178.7 | 80.5 | −62.5 | −169.0 | 53.1 | −70.4 |
| | (12.4) | (3.0) | (4.2) | (12.4) | (1.6) | (3.0) | (12.0) | (4.2) | (2.3) |
| 3*S*,4*S* | 59.8 | −50.6 | −165.4 | 61.3 | −33.9 | −175.8 | 73.9 | −59.6 | 175.3 |
| | (3.3) | (4.5) | (11.7) | (3.2) | (7.1) | (12.3) | (1.9) | (3.3) | (12.3) |
| 3*R*-H,1-C | −55.0 | −59.1 | −36.0 | −173.7 | −167.8 | −163.1 | 62.7 | 43.2 | 59.3 |
| | (2.0) | (1.7) | (3.7) | (6.7) | (6.5) | (6.3) | (1.4) | (3.1) | (1.7) |
| 3*R*-H,5-C | 51.2 | −60.7 | 179.6 | 52.4 | −42.7 | 168.7 | 65.5 | −72.9 | 161.0 |
| | (2.4) | (1.5) | (6.8) | (2.3) | (3.2) | (6.6) | (1.2) | (0.8) | (6.2) |
| 3*S*,H,1-C | 58.1 | 53.4 | 76.2 | −59.6 | −54.9 | −49.8 | 176.1 | 155.5 | 172.0 |
| | (1.8) | (2.2) | (0.7) | (1.6) | (2.1) | (2.5) | (6.8) | (5.7) | (6.7) |
| 3*S*-H,5-C | −61.5 | −171.6 | 69.8 | −60.2 | −153.5 | 58.3 | −47.2 | 177.4 | 49.8 |
| | (1.5) | (6.7) | (1.0) | (1.6) | (5.6) | (1.8) | (2.7) | (6.8) | (2.5) |

[a] The coupling constant values $^3J_{HH}$ and $^3J_{HC}$ were calculated by using Karplus-type equations: $^3J = A\cos^2\phi + B\cos\phi + C$ with different coefficients in the homonuclear case,[41,42] ($^3J_{HH}$) $A = 9.5$, $B = -1.3$, and $C = 1.6$, and in the heteronuclear case,[30] ($^3J_{HC}$) $A = 5.7$, $B = -0.6$, and $C = 0.5$.

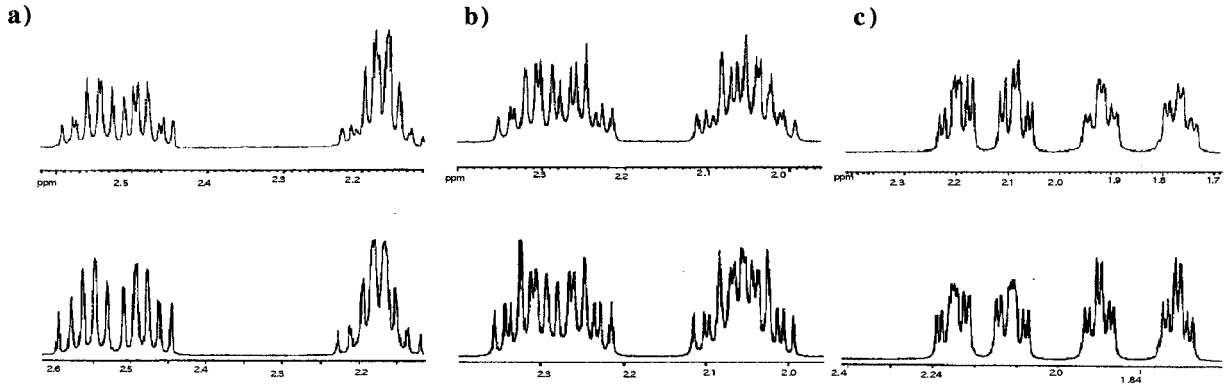


**Figure 3.** (top) Details of the 500 MHz $^1$H spectrum of **2M** in $D_2O$ (a) at pH 4 (**21M**), (b) at pH 7 (**22M**), and (c) at pH 10 (**23M**). (bottom) Simulation of the signals using the NMRII software, 500 MHz, and line width 0.5 Hz (the coupling constants were evaluated by simulation and iteration using the Bruker PANIC software).

**(b) Coupling Constants.** Analysis of the $^1$H NMR $^3J$ values was used to establish the major solution-state conformation of 2-methylglutamic acid. Surprisingly, in solution, the backbone of this analogue is found to be relatively rigid, and it would thus be expected that much stereochemical and conformational data could be deduced from the $^1$H,$^1$H and $^{13}$C,$^1$H coupling constants.

The geminal protons were found to be inequivalent, and the spin system is complex. The first-order analysis of the spin system was confirmed by spectral simulation: the subspectra calculated from the $J$ and $\delta$ values in Tables 2 and 3 are in agreement with the experimental data (Figure 3). As the protons H(3a), H(3b), H(4a), and H(4b) constituted a highly coupled system, the coupling constants could be evaluated by NMR simulation and iteration (Bruker PANIC software) using the NMR data at 500 MHz. On this basis, it is possible to simulate the four-spin system **A**−**D** highly coupled using Bruker PANIC software; the results are well correlated with the experimental findings and the values of coupling constants at different pH values are shown in Table 2 and at different temperatures in Table S1 of Supporting Information. The experimental and simulated four-spin system of 2-methylglutamic acid at different pH values are shown for comparison in Figure 3 and at different temperatures in Figure S1 of Supporting Information.

Determination of heteronuclear long-range $^{13}$C−$^1$H coupling constants by the selective 2D INEPT experience[37] is especially helpful in order to inquire about the relative position of the (α-$CO_2^-$, γ-$CO_2^-$, α-Me) with respect to the backbone. The homonuclear and heteronuclear three-bond coupling constants of the **2M** compound are also necessary for the assignments of the diastereotopic protons at C(3) and C(4).

Heteronuclear $^{13}$C−$^1$H coupling constants in acidic and basic solution are difficult to measure because of overlapping $^1$H multiplets and problems encountered with $T_2$ relaxation. Thus, it is not possible to evaluate the population of rotamers corresponding to the $\chi 1$ rotor in these cases (**21M**, **23M**), and only the $^3J_{^1H^1H}$ coupling constants are used to determine the populations of the rotamers about $\chi 2$. This results are summarized in the Table 2.

**(c) Conformational Analysis.** The reliable analysis of spin−spin coupling constants and chemical shifts of the system was elucidated in comparison with spectrum simulation. The use of vicinal spin−spin coupling for the studies of molecular conformation relies on a general relation between the size of the spin−spin coupling constant $^3J$ and the intervening torsion angles $\chi 1$ and $\chi 2$.

In small structures such as the 2-methylglutamate, side-chain atoms are allowed to rotate freely around the $\chi$ dihedral

angles. NMR parameters should therefore be interpreted in terms of contribution from the staggered conformations corresponding to $\chi$ values of 180, −60, and 60° (rotamers **A**−**C** and **a**−**c**). The population of these three rotamers is determined from NMR ($^3J_{HH}$ and $^3J_{HC}$ coupling constants), and the calculated coupling constants ($^3J_{HH}$ and $^3J_{HC}$) in gauche and anti conformations are represented in Figure 2 by using Karplus-type equations.[31,38−40] These populations are given for the two dihedral angles $\chi$1 and $\chi$2 in Table 2. The distinction between rotamers is only possible if the stereospecific assignment for $\beta$-protons is available.

The constant $^3J_{H_3H_4}$ gives information about the values of dihedral angle $\chi$2. Thus, it is possible to interpret these values as population of the three rotamers **a**−**c**.

$$^3J_{H3aH4a} = P_aJ_t + P_bJ_g + P_cJ_g$$

$$^3J_{H3bH4b} = P_aJ_t + P_bJ_g + P_cJ_g$$

$$P_a + P_b + P_c = 1$$

The values of $J_g$ and $J_t$ designated the theoretical coupling constants $^3J_{3,4}$ for the protons H(3) and H(4) in gauche and anti conformation represented in the Newman projection (Figure 2). The most widely used values are those calculated using Karplus-type equations: $^3J = A\cos^2\phi + B\cos\phi + C$ with different coefficients in the homonuclear case,[41,42] $A = 9.5$, $B = -1.3$, and $C = 1.6$, and in the heteronuclear case,[30] $A = 5.7$, $B = -0.6$, and $C = 0.5$, approximately $J_g = 3.3$ Hz, $J_t = 12.4$ Hz, for $^3J_{HH}$ and $J_g = 1.8$ Hz, $J_t = 6.5$ Hz, for $^3J_{HC}$. In what follows, the theoretical values of these conformationally informative coupling constants are calculated from torsion angles computed by MD for **2M** (Table 3) and will thus be related to the rotamer populations. It appears that rotamer populations accurate to ±10% can still be obtained.

For the dihedral angle $\chi$2, the coupling constants of 10.3 Hz measured on the H(3a) and simultaneously on the H(3b) protons ($^3J_{H3aH4a}$ and $^3J_{H3bH4b} = 10.3$ Hz) provide evidence for the identification of the major rotamer. From these values, we can deduce the position of the corresponding protons in the Newman projection. It can be seen that the two coupling constants $^3J_{H3aH4a}$ and $^3J_{H3bH4b}$ are nearly identical. These values are only in good agreement with the calculated coupling constants of the torsion angle $\chi$2, in the anti conformation **a**. The differences, which are not really larger than the experimental error (0.3 Hz), can be interpreted as a slight variation of the dihedral angles around C(3)−C(4) (155°) or rather, as a slight contribution of the *gauche* conformation, which is approximately evaluated by the equation $3.3(1 - \alpha) + 12.4\alpha = 10.3$ (80% anti and 20% gauche).

The temperature dependence of coupling constants are shown in Table S1. The side chain of the 2-methylglutamate is found in the same predominant conformation *t*-**a**, based on the analysis of the vicinal $^3J_{H_3H_4}$ coupling constants. The values of homo and heteronuclear long-range $^3J_{HH}$ and $^3J_{HC}$ are used for the following:

(i) To attribute the conformation **A**, **B**, or **C**. Thus, our measured values (Table 2) of $^3J_{H3aC5}$ and $^3J_{H3bC5} \leq 2$ Hz should confirm the large participation of conformation *t*-**a** for the torsion angle $\chi$2. This experiment was the unique possibility to explore the position of the different substituents about the torsion angle $\chi$1. The $^3J_{H3aC1} = 1.4$ Hz, $^3J_{H3aC(2Me)} = 2.6$ Hz and in another part $^3J_{H3bC1} = 5.2$ Hz, $^3J_{H3bC(2Me)} = 1.5$ Hz should include a large participation of conformation **C** for this torsion angle $\chi$1 (Figure 2).

(ii) To resolve the ambiguity to find the configuration pro-*R* or pro-*S* of the proton H(3a).[31,38−40] The $^{13}C-^1H$ coupling constants are "out of phase" with the $^1H-^1H$ coupling constants so that in rotamer **C** (Figure 2a), for example, $H(3)_{pro\text{-}R}$ and $H(3)_{pro\text{-}S}$ are gauche and trans, respectively, to the carboxyl carbon C(1), but are both gauche to the carboxyl carbon C(5) in rotamer **a** (Figure 2b). The experimental NMR data from H(3) are measured for **2M** at pH 7 (**22M**), $^3J_{C(5)H(3a)}$ (2 Hz), $^3J_{C(5)H(3b)}$ (2 Hz), $^3J_{C(1)H(3a)}$ (1.4 Hz), and $^3J_{C(1)H(3b)}$ (5.2 Hz) and, thus, the $H(3)_{pro\text{-}R}$ is assigned to H(3a) and $H(3)_{pro\text{-}S}$ to H(3b). The most important coupling constants involve the C atom of methyl group, of 1- and 5-carboxylate groups ($\alpha$ or $\gamma$); their long-range couplings allow the assignment of the diastereotopic protons of the adjacent methylene group. The homonuclear and heteronuclear three-bond coupling constants, necessary for the assignments of the diastereotopic protons at C(3) and C(4), are listed in Table 2.

Qualitative considerations may be applied as follows to achieve diastereotopic assignment of the methylene protons. The $\chi$1 angle can be restricted to *t*-**A** when the two $^3J_{H3aC1}$ and $^3J_{H3bC1}$ coupling constants are small (both should be ∼2 Hz). If one large (5−6 Hz) and one small coupling are observed, both $g^+$-**B** and $g^-$-**C** are possible for $\chi$1. Additional information is needed to distinguish between these two last cases. This may be accomplished using the heteronuclear $^3J_{NH3a}$ and $^3J_{NH3b}$ coupling constants. Two patterns are possible for the N−H(3) cross-peaks of the rotamers about $\chi$1. One strong and one weak (or even invisible) peak are expected for both $H(3)_{pro\text{-}S}$ and $H(3)_{pro\text{-}R}$. Thus, the discrimination between the rotamers **B** and **C** is only possible if the protons H(3a) and H(3b) or H(4a) and H(4b) are attributed stereospecifically. This attributes $H(3a)_{pro\text{-}R}$ and $H(3b)_{pro\text{-}S}$ is obtained by analyzing all the coupling constants values $^3J_{^{13}C^1H}$ and $^3J_{^1H^1H}$ from H(3a) and H(3b) and also by an inverse $^1H$, $^{15}N$ long-range experiment. We can observe an enhancement only of the signal corresponding to the H(3a) proton, which allows us to demonstrate the stereospecificity of $H(3a)_{pro\text{-}R}$ and to conclude that the conformation $g^-$-**C** is predominant.

A stereospecific attribution is then possible for the H(4) protons as the two spin−spin coupling constants $^3J_{3a4a}$ and $^3J_{3b4b}$ are 10.3 Hz and in good agreement with the calculated coupling constants for the rotamer *t*-**a** relative to the torsion angle $\chi$2. Thus H(4a) and H(4b) could be attributed as $H(4)_{pro\text{-}S}$ and $H(4)_{pro\text{-}R}$, respectively.

All these observations may be rationalized by the presence of a preferred conformation **C** relative to the torsion angle $\chi$1 and *t*-**a** relative to the torsion angle $\chi$2 (Figure 2), in which the 2-methyl group and the protons H(3) are in spatial proximity relative to the alkyl chain and in which all the homonuclear and heteronuclear coupling constants are in good agreement.

It is concluded, from NMR data, that the 2-methylglutamic acid exists in solution as two major rotamers $g^-$-**C** and *t*-**a**, with the less steric hindrance but without any electrostatic interactions as for other analogues previously studied. Other

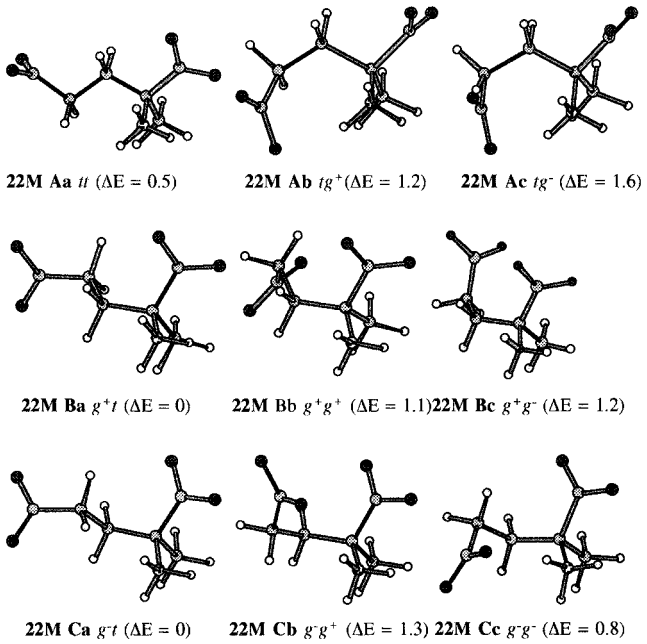


**Figure 4.** The nine conformations of **22M** represented at pH 7.

minor conformation could also participate a little in solution, such as $g^+$-**B** or *t*-**A** and $g^+$-**b** and $g^-$-**c**. The preferred conformation is the sterically favored one, *t*-**a** ($\gamma$-$CO_2^-$ and side chain trans), but a conformational equilibrium between conformers $g^+$-**b** and $g^-$-**c** occurs ($\gamma$-$CO_2^-$ and side chain gauche), these conformers being very likely stabilized by an electrostatic interaction between the α-amino and the $\gamma$-carboxylate (Figure 4).

The most important parameters for the determination of 3D structure are *J* coupling constants, NOE-derived distances, and chemical shifts. A coupling constant may result from several possible dihedral angles, as indicated by analysis of the Karplus curve. Therefore, most structures have been determined by the use of MD simulations. The agreement of the generated structures with the coupling constants is then examined (Table 3).

**Second Part: Molecular Modeling.** We performed computational chemical methods (molecular dynamics and molecular mechanics calculations), starting with the structure of glutamic acid for the simulation of **2M**, with removal conversion of the α-$NH_3^+$ and $\gamma$-$CO_2^-$ groups by α-$NH_2$ (**23M**) and $\gamma$-$CO_2H$ (**21M**) modified functional groups. Charges and atomic potentials were then redefined for the new molecules using the built-in algorithm of the program. The structures were minimized, in "steepest descent" and "conjugate gradients" steps, until convergence (Figure 4). Electrostatic interactions are calculated in the force field by a Coulombic expression. The final structures obtained after several calculations were examined for the overall energetic favorability and compared with the structure derived from the NMR data.

A good procedure for choosing the appropriate force field to identify the experimentally determined conformation as the lowest energy structure is to fit the parameters of the interaction function to results (potential or field) of *ab initio* quantum calculations on a small molecular cluster. However, the alternative is to fit the force field parameters to experimental data like, in our case, NMR data. The ability of the CVFF force field to reproduce the experimental, NMR-determined conformations of the other structural analogues[21] has suggested to us that the Biosym CVFF force field was

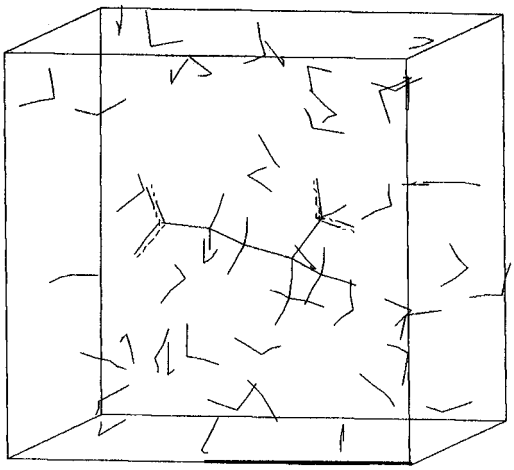

**Figure 5.** Solvation box containing the **2M** molecule and several water molecules (**2M** + 48$H_2O$) to mimic the solvent effect with explicit modeling of water in molecular dynamics protocol.

an adequate tool for modeling the **2M** compound. We used the CVFF force field from Dauber-Osguthorpe[43] in which cross-terms represent the coupling of the deformations of internal coordinates and describe the coupling between adjacent bonds. These terms are required to reproduce accurately experimental vibrational frequencies and, therefore, the dynamic properties of molecules. A Morse function was used to describe the stretching of bonds.

A widely used method to mimic the solvent screening effect is to use a distance-dependent relative permittivity $\epsilon = r$, leading to an $r^2$ dependence of the Coulombic energy.[44] But in previous studies[19] to model explicitly the solvent effect, we have used the electrostatic interaction expression $E = Kq_1q_2/\epsilon r$ and have adjusted the relative permittivity to a value $\epsilon = 5$ corresponding to the interactions in aqueous solution. For the first time, a protocol is conceived that would rapidly give results in conformational studies, avoiding the introduction of explicit water molecules (with $\epsilon = 78$ and 5), but it seems better to mimic the solvent with explicit modeling of water. Then, we have constructed solvation boxes around the charged end groups of the molecules containing several water molecules by using boundary conditions. A cutoff function of 15 Å was applied for nonbonded interactions. The relative permittivity was set to $\epsilon = 1$ and a box contained 48 (12-12-12) water molecules. However, it is not of practical use: the energies obtained are those of **22M** + 48$H_2O$ systems (Figure 5); thus, the energies of the minimized **22M** molecules themselves are very difficult to evaluate. A protocol was used (with $\epsilon$ values and with explicit solvent molecules incorporated during the run). Then, when a good agreement between theoretical (MD) and experimental (NMR) data was obtained, nothing else was changed in the force field, considering that it was well-fitted.

**Molecular Mechanics.** The different conformations of the **2M** isomers are minimized by molecular mechanics. The energies obtained (using a dielectric constant fixed to $1 \leq \epsilon \leq 5$, $\epsilon = 4r$, and $\epsilon = 78$) are reported in Table 4. The relative population of the *i*th conformational state, $P_i$ with energy $E_i$, is dictated by the Boltzmann distribution,

$$P_i = \exp(-E_i/kT)/\sum \exp(-E_i/kT)$$

We have calculated the population of different conformations using Maxwell−Boltzmann statistics. Upon direct minimi-

**Table 4.** Energies ($E_{pot}$, kcal mol$^{-1}$) and Boltzmann Probabilities (BP, %) of the Nine Lowest Energy Conformations for the **2M** Isomer by Molecular Mechanics[a]

| | **22M** ($\epsilon = 5$) | | **22M** ($\epsilon = 78$) | | **22M** (water box)[b] | | **21M** ($\epsilon = 5$) | | **23M** ($\epsilon = 5$) | |
|---|---|---|---|---|---|---|---|---|---|---|
| | $E_{pot}$ | BP | $E_{pot}$ | BP | $E_{pot}$ | BP | $E_{pot}$ | BP | $E_{pot}$ | BP |
| Aa | −7.6 | 0 | 9.2 | *14* | −638 | 0 | −5.6 | *11.5* | 19.9 | *46* |
| Ab | −11.7 | *91* | 10.1 | 3 | −692 | 0 | −4.9 | 3.5 | 31.0 | 0 |
| Ac | −8.4 | 0 | 10.7 | 1 | −679 | 0 | −4.5 | 2 | 21.9 | 2 |
| Ba | −6.9 | 0 | 8.6 | *43* | −659 | 0 | −6.2 | *32* | 20.0 | *39* |
| Bb | −5.8 | 0 | 10.2 | 3 | −684 | 0 | −5.1 | 5 | 22.1 | 1 |
| Bc | −1.5 | 0 | 9.8 | 6 | −686 | 0 | −5.0 | 4 | 26.9 | 0 |
| Ca | −7.1 | 0 | 8.9 | *24* | −699 | *100* | −6.2 | *32* | 20.7 | 12 |
| Cb | −3.4 | 0 | 10.2 | 2 | −379 | 0 | −4.8 | 3 | 27.8 | 0 |
| Cc | −10.3 | 9 | 9.9 | 4 | −686 | 0 | −5.3 | 7 | 23.5 | 0 |

[a] $\epsilon$ is the dielectric constant used in the force field equations. The major populations are in italics. [b] The energy obtained are those of "molecule + 48 $H_2O$" systems ($\epsilon = 1$).

zation of **22M** with $\epsilon = 5$, an overestimated electrostatic attraction between the α-$NH_3^+$ and the γ-$CO_2^-$ groups leads to the lowest energy structure Ab (Table 4). The Boltzmann calculations (Table 4) indicate that conformation Ab should have the highest populations (91%), compared to the others low-energy conformers, but this is not entirely coherent with the NMR results. It is possible to try to adjust the relative permittivity to a value between 1 and 78 and thus reproduce the NMR solution. So, if we reduce the electrostatic contribution on **22M** by using $\epsilon = 78$ or by removing one formal charge, on the γ-carboxylate group (the case of **21M** at isoelectric pH 3, with the zwitterionic form γ-$CO_2H$) or on the amino group (the case of **23M** at pH 11), the Boltzmann probabilities generate the approximate ratios of minimum-energy conformations available for **22M** in aqueous solution at pH 7. At pH 3 and 11, the electrostatic interactions are sufficiently reduced and Aa, Ba, and Ca conformations are sterically favored. The correspondence between the calculated populations of rotamers and the NMR experimental data (Table 2; **A**, 15; **B**, 15; **C**, 70; **a**, 75; **b**, 10; **c**, 15) is improving but is not perfect. For this charged and flexible molecule, it is obvious that MD studies may have to be used to get more reasonable statistical participation of every structures to improve the NMR result.

**Molecular Dynamics.** To simulate the molecular movements in solution, different protocols of molecular dynamics have been used, with the Biosym software INSIGHTII and DISCOVER.

In MD calculations, Newton's equation of motion is solved with forces calculated from a force field (CVFF) consisting of terms for bond stretching, bond angle and dihedral angle deformation, chiral restraints, and nonbonded interactions.[36,45] The empirical force field methods are capable of producing a collection of structures that span all the accessible conformational space of the molecule. In order to find suitable parameters (solvent and electrostatic term, number of water molecules, times, temperature) for simulation of this specific molecule, we varied them systematically and performed 60 simulations (Tables 5 and 6 and Table S2 of the Supporting Information).

We have run experiments starting from each one of the nine possible conformations of the three compounds (**21M**, **22M**, **23M**) to compare their energies and to determine their frequency in the interconversion. The results are summarized in Figure 4 and in Tables 5 and 6.

(i) Conformational analysis of this amino acid begins with the simple assumption of one dominating conformation *t*-**a** for χ2 but remains an ambiguity about χ1 as only a qualitative presumption gives the major rotamer $g^-$-**C** and no $^3J_{HH}$ NMR data are measured for this dihedral angle. MD performed with "a distance-dependent dielectric, $\epsilon = R_{ij}$" ($\epsilon = 5$ and $\epsilon = 70-78$) using the nine different starting structures (obtained by combined incrementation of the side-chain bonds χ1 and χ2) yields the first crude averaged solutions (Tables 5 and 6).

(ii) Each structure is further refined by putting the molecule (**22M**) in a solvent box of $H_2O$.[45] The results obtained show a concentration-dependent hydration number for this small charged molecule. The best procedure uses a cube of volume $12 \times 12 \times 12$ Å$^3$ containing 48 water molecules (Figure 5) to allow periodic boundary conditions and a nonbonded cutoff distance of 15 Å.

The purpose of this work is to try to reproduce experimentally NMR-obtained structural results by simulation methods and to study these very charged systems to give some insight into the water exchange on the three ions. The simulations were carried out on systems **22M** containing one positive ammonium ion and two negative carboxylate ones and a reasonable number of water molecules (48). The intermolecular interactions are assumed to be pairwise additive. Because of the presence of the methyl group on the same carbon that bears ammonium and carboxylate groups, the hydration of the molecule is mainly governed by electrostatic and steric factors to represent (or consider) the water−water intermolecular interactions, the ion−water interaction, and the ligand−field effects.

**Systematic Searches.** For these small molecules, the computational method has the advantage of searching the conformational space most completely. In what follows we will describe in detail the application of systematic methods in attempting to generate a realistic description of molecular structures in solution. Of considerable interest is the variation of the potential energy of **2M** with rotation about C(2)−C(3) and about C(3)−C(4). The energy diagram is shown in Figure 6a, for χ2 relative to *t*-**a** and for χ1 relative to *t*-**A**, as calculated by a systematic search using $\epsilon = 78$. The global energy minimum is found for the *t*-**a** conformer, while local minima, located very close to the fully staggered gauche $g^+$-**b** conformer are 5 kcal mol$^{-1}$ above the global minimum. As the two C−C bonds are allowed to rotate, the potential energy of the **2M** molecule will be represented in Figure 6b by a hypersurface in a three-dimensional space defined by the three orthogonal axes $\Delta E$, χ1, and χ2. The topological features of this conformational hypersurface have

**Table 5.** Simulations for the Nine Conformations of the **2M** Isomer at Different pH (**21M**, **22M**, **23M**)[a]

| | 200 ps simulations at 300 K with $\epsilon = 5$ starting conformations | | | | | | | | | frequency | |
|---|---|---|---|---|---|---|---|---|---|---|---|
| | Aa | Ab | Ac | Ba | Bb | Bc | Ca | Cb | Cc | total | % |
| **21M** | | | | | | | | | | | |
| Aa | | | | x (193) | | | | (200) | | 393 | 22 |
| Ab | | | | x (5) | | | | | | 5 | 0 |
| Ac | | | | x (2) | | | | | | 2 | 0 |
| Ba | | | | | | x (178) | | | | 178 | 10 |
| Bb | | | | | | x (18) | | | | 18 | 1 |
| Bc | | | | | x (200) | x (4) | | | | 204 | 11 |
| Ca | x (148) | x (195) | x (200) | | | | x (200) | | x (194) | 937 | 52 |
| Cb | x (8) | x (4) | | | | | | | x (2) | 14 | 1 |
| Cc | x (44) | x (1) | | | | | | | x (4) | 49 | 3 |
| **22M** | | | | | | | | | | | |
| Aa | | | | | | | | | | 0 | 0 |
| Ab | | x (200) | | | x (193) | | | | | 393 | 22 |
| Ac | | | x (200) | | x (7) | | | | | 207 | 11 |
| Ba | x (200) | | | x (200) | | x (199) | | | | 599 | *34* |
| Bb | | | | | | x (1) | | | | 1 | 0 |
| Bc | | | | | | | | | | 0 | 0 |
| Ca | | | | | | | | x (22) | | 22 | 1 |
| Cb | | | | | | | | | | 0 | 0 |
| Cc | | | | | | | x (200) | x (178) | x (200) | 578 | 32 |
| **23M** | | | | | | | | | | | |
| Aa | x (199) | | x (188) | | | x (196) | x (196) | | | 779 | 44 |
| Ab | | | | | | | x (1) | | | 1 | 0 |
| Ac | x (1) | | x (12) | | | (4) | x (3) | | | 20 | 1 |
| Ba | | | | x (198) | x (185) | | | | | 383 | 21 |
| Bb | | | | x (2) | x (15) | | | | | 17 | 1 |
| Bc | | | | | | | | | | 0 | 0 |
| Ca | | x (200) | | | | | | x (200) | x (194) | 594 | *33* |
| Cb | | | | | | | | | | 0 | 0 |
| Cc | | | | | | | | | x (6) | 6 | 0 |

[a] Each column represents one simulation. "x" indicates that conformation was found, and frequency is given in parentheses. Frequency is the number of times each conformation is found. The percentage of each conformation deduced from its frequency is reported in Table 6.

**Table 6.** Results of the MD Simulations Using the Different Protocols[a]

| | protocol[b] for **2M** | | | | | | | | | | | |
|---|---|---|---|---|---|---|---|---|---|---|---|---|
| | 1 | | | 2 | | | 3 | | 4 | | 5 | 6 |
| | **21M** | **22M** | **23M** | **21M** | **22M** | **23M** | **21M** | **22M** | **21M** | **22M** | **22M** | **22M** |
| Aa | 17 | 1 | 30 | 22 | 0 | 44 | 24 | 11 | 38 | 21 | 9 | 22 |
| Ab | 8 | 44 | 3 | 0 | 22 | 0 | 19 | 1 | 6 | 0 | 4 | 0 |
| Ac | 6 | 0 | 1 | 0 | 11 | 1 | 2 | 2 | 1 | 1 | 0 | 0 |
| Ba | 10 | 1 | 23 | 10 | 34 | 21 | 6 | 43 | 33 | 34 | 40 | 42 |
| Bb | 14 | 10 | 3 | 1 | 0 | 1 | 2 | 1 | 0 | 11 | 3 | 0 |
| Bc | 3 | 0 | 0 | 11 | 0 | 0 | 14 | 0 | 0 | 0 | 3 | 0 |
| Ca | 38 | 5 | 40 | 52 | 1 | 33 | 23 | 4 | 19 | 21 | 30 | 31 |
| Cb | 0 | 0 | 0 | 1 | 0 | 0 | 1 | 11 | 1 | 12 | 1 | 0 |
| Cc | 4 | 39 | 0 | 3 | 32 | 0 | 9 | 27 | 2 | 0 | 10 | 5 |
| | Populations of Rotamers about $\chi 1$ and $\chi 2$ | | | | | | | | | | | |
| **A** | 31 | 45 | 34 | 22 | 33 | 45 | 45 | 14 | 45 | 22 | 13 | 22 |
| **B** | 27 | 11 | 26 | 22 | 34 | 22 | 22 | 44 | 33 | 45 | 46 | 42 |
| **C** | 42 | 44 | 40 | 56 | 33 | 33 | 33 | 42 | 22 | 33 | 41 | 36 |
| **a** | 65 | 7 | 93 | 84 | 35 | 98 | 53 | 58 | 90 | 76 | 79 | 95 |
| **b** | 22 | 54 | 6 | 2 | 22 | 1 | 22 | 13 | 7 | 23 | 8 | 0 |
| **c** | 13 | 39 | 1 | 14 | 43 | 1 | 25 | 29 | 3 | 1 | 13 | 5 |

[a] Percentage of each conformations generated with different protocol starting from the nine different conformations (for each isomer 1800 structures were examined). [b] Protocols: (1) 50 ps MD run at 300−600 K with $\epsilon = 5$; (2) 200 ps MD run at 300 K with $\epsilon = 5$; (3) 50 ps MD run at 300−600 K with $\epsilon = 70$; (4) 200 ps MD run at 300 K with $\epsilon = 70$; (5) 50 ps MD run at 300−600 K in a water box; (6) 200 ps MD run at 300 K in a water box.

been analyzed in Figure 6c. The global minimum is that shown in Figure 6c (−60/180), as are local minima (e.g., 180/180). The highest energy peak is (0/0, 40 kcal mol$^{-1}$), while a number of other maxima exist (e.g., 120/0). The hypersurface is also characterized by a number of saddle points (e.g., 0/60 and 120/60) which are the maxima in Figure 6b and of super saddle points (e.g., 60/0 and 180/0). Figure 6 illustrates the behavior of the **2M** molecule with two degrees of conformational freedom.

**Preliminary Protocol.** For an exploration of the conformational space, after an equilibration period of 8 ps, the dynamics are run at 300 K with periodic jumps to 600 K to supply the system with energy (to pass conformational barriers). The 50 ps trajectory is sampled every picosecond; the structures are then minimized by molecular mechanics and stored. The stability of the different conformers of **21M**, **22M**, and **23M** has been tested by a 200 ps dynamics protocol at 300 K.

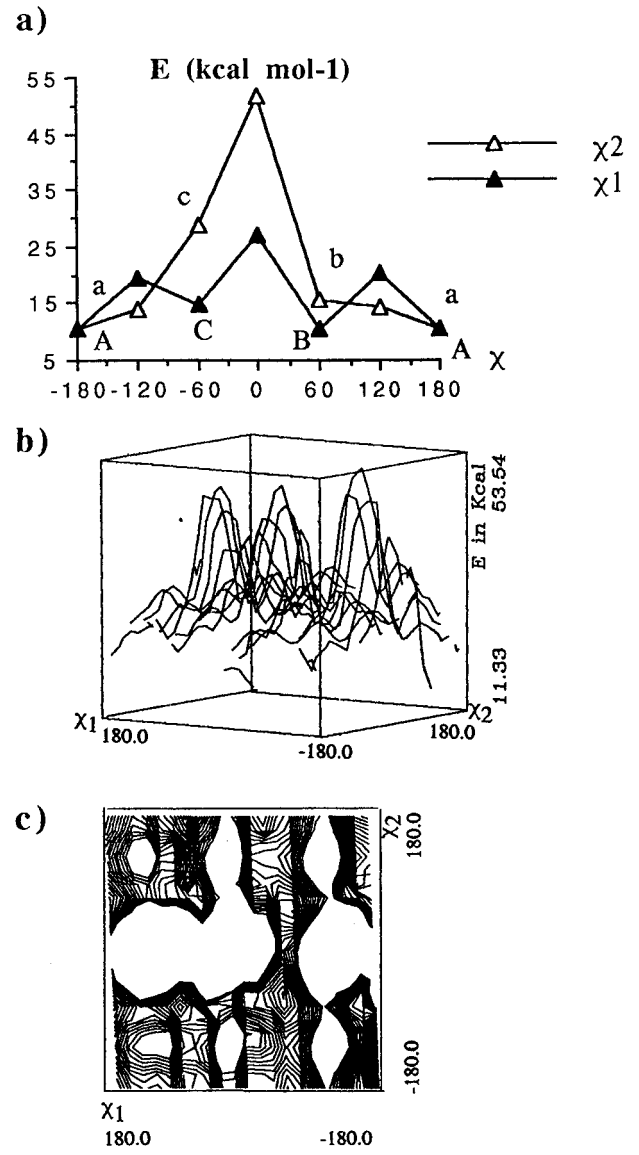


**Figure 6.** (a) Potential energy of **2M** central C(2)−C(3) and C(3)−C(4) rotation with the substituents groups held staggered ($\chi 2 = \chi 1 = 180°$) during the rotation of $\chi 1$ and $\chi 2$, respectively). (b) Representation of the **2M** by a hypersurface in a three-dimensional space defined by the three orthogonal axes $\Delta E$ $\chi 1$, and $\chi 1$. (c) The topological features of this conformational hypersurface have been analyzed.

The important electrostatic ($\alpha$-$NH_3^+$ and $\gamma$-$CO_2^-$ groups) and steric (methyl group and intermediate eclipsed forms) contributions lead to a very good stabilization of some conformations and hinder an interconversion of the corresponding rotamers since the energetic barriers are too high. No interconversion is observed from **22M** Ba, Ca, Cb, and Cc at 600 K ($\epsilon = 70$) and from **22M** Aa, Ba, and Ca at 500 K (hydration boxes).

The major structure is almost the same (Table 6) either at 300 K or at 300−600 K according to one MD protocol. If the temperature increases, this allows conformational changes to take place on the time scale of molecular dynamics simulations, Ca → Cc → Ac → Ab → Aa; thus, the Aa conformation is favored (Figure 7a). At high temperature, the molecule explores more states; however, the fraction of time it spends near the lowest energy states is smaller. The long MD trajectories (200 ps) at 300 K with hydration boxes will be more efficient to find **2M** conformations than stochastic methods (300−600 K, 50 ps).

**MD Protocols.** To find an optimal protocol for better sampling and statistical evaluation, another factor has to be considered, the time of the MD run. This should be sufficient to sample all of the conformational space. A long MD (800 ps) is performed on Ca (Figure 7b), Aa, and Ba at 300 K (hydration boxes). For all these dynamics experiments, the starting conformers Aa, Ba, and Ca appear very stable along the MD trajectories, but each of the three structures leads to ~2% of a different minor conformer corresponding to Cb (from Ca), Bc (from Ba), and Ba (from Aa). That has encouraged us to use the method of multiple starting points[46] in order to better sample phase space. MD runs were achieved for the nine possible minimized conformations of **2M** isomer. These nine minimized conformations were then used as the starting structures, for a 200 ps MD run at 300 K with $\epsilon = 5$ and 70 and for simulations with water as a solvent. The frequency (how many times we get the same conformation) deduced from the different structures are reported at different pH values with $\epsilon = 5$ in Table 5 and with $\epsilon = 70$ or in water box in Table S2 of the Supporting Information.

The equilibration period that is required will depend on the relaxation time of some properties such as the kinetic energy, which requires short (picosecond) equilibration times, whereas dielectric properties may require longer times of the order of ten of picoseconds.[45] Protocol 4 (200 ps MD run at 300 K with $\epsilon = 70$) with 8 ps of equilibration time generates 20% Aa, 34% Ba, 9% Ca, and 22% Cb (plus 2% Ab and 13% Cc) while the same protocol 4 with 4 ps of equilibration time generates 21% Aa, 34% Ba, 21% Ca, and 12% Cb (plus 1% Ac and 11% Bb). Thus, the results will be generally analyzed by taking averages over simulations with different initial conditions.

To compute NMR parameters from the simulation results (Table 6), some type of averaging is required. Many of the conformational properties are not linearly related to the conformations (i.e., NOEs and *J* couplings) and need to be calculated for each structure (Table 3) and then averaged (Table 7).[40]

Averaging is required to correctly predict properties for a population of low-energy computer models distributed over *P* conformational states. By using $P_i$, the fractional population for each *i*th conformational microstate, the average coupling constant can be computed from

$$^3J_{HH} = \sum P_i \, ^3J_{iHH}$$

And for the coupling constants $^3J_{HC}$

$$^3J_{HC} = \sum P_i \, ^3J_{iHC}$$

The coupling constants were calculated from the corresponding dihedral angles of each conformer generated by molecular dynamics (Table 3).

Experimental values (Table 2) are discussed with regard to the calculated values in these different conformers (Table 7) from the lowest structures in energy. So, the conformational equilibrium possible in solution is taken into account in these averaging procedures. For example, in Table 7, the coupling constants $J_{H,H}$ evaluated for the conformer population generated by the protocol 2 show that **2M** solution averaging is well described (22% Aa, 10% Ba, 52% Ca, 11%

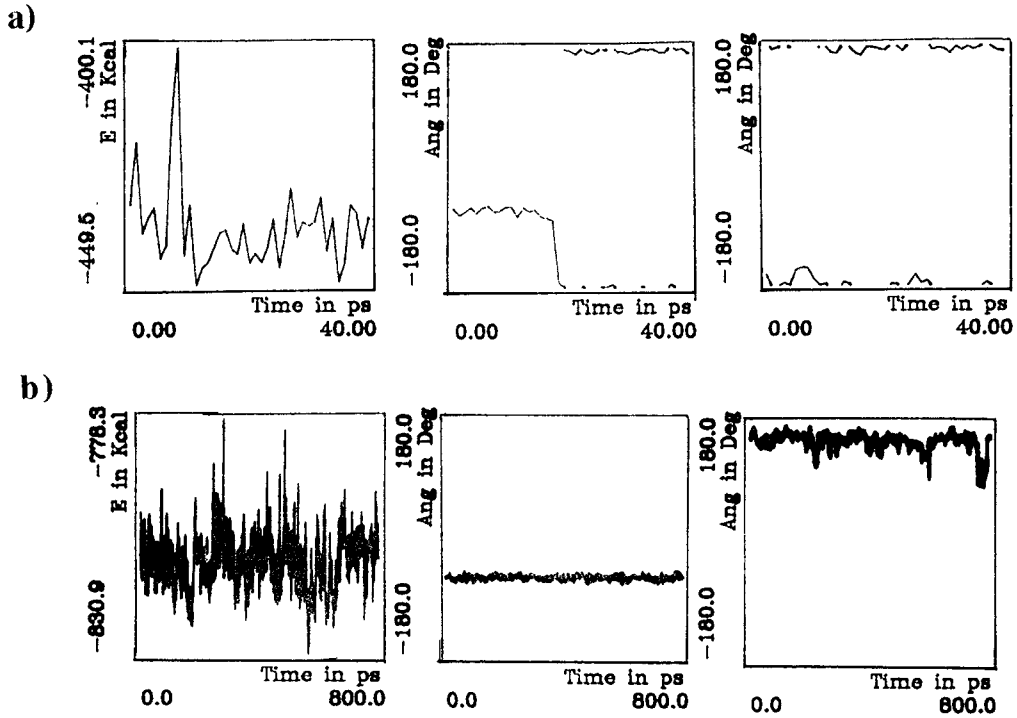


**Figure 7.** Trajectories of some characteristic homonuclear dihedral angles and heteronuclear dihedral angles relative to $\chi 1$ and $\chi 2$ for **2M** isomer at pH 7 by MD simulation with solvation box: (a) with temperature jump (300−600 K); (b) during a long time scale (800 ps) at constant temperature (300 K).

**Table 7.** Homonuclear ($^1$H−$^1$H) and Heteronuclear ($^{13}$C−$^1$H) Coupling Constants in $D_2O$ Used in the Conformational Analysis of the **2M** Isomer

| | $J_{exp}$ (NMR) | | | $J_{calc}$(MD)/Hz | | | | | |
|---|---|---|---|---|---|---|---|---|---|
| | **21M** pH 3 | **22M** pH 7 | **23M** pH 11 | **21M**[b] | **23M**[c] | **22M**[d] | **22M**[e] | **22M**[f] | **22M**[g] |
| $^3J_{HH}$ | | | | | | | | | |
| 3a, 4a | 9.3 | 10.0 | 11.6 | 10.5 | 12.0 | 10.1 | 9.1 | 10.1 | 11.7 |
| 3a, 4b | 7.4 | 6.5 | 4.8 | 3.7 | 2.8 | 4.8 | 5.2 | 4.0 | 3.0 |
| 3b, 4a | 7.0 | 5.7 | 5.0 | 3.9 | 2.7 | 3.5 | 4.3 | 4.2 | 3.3 |
| 3b, 4b | 9.2 | 10.3 | 12.1 | 10.7 | 12.0 | 10.1 | 9.0 | 10.2 | 11.7 |
| $\sum\Delta J_{HH}$ MD/NMR (pH 7) | | | | 5.5 | 10.4 | 4.2 | 4.9 | 4.2 | 9.0 |
| $\sum\Delta J_{HH}$ MD/NMR (pH 3) | | | | 9.5 | 14.4 | 7.8 | 5.3 | 8.0 | 13.0 |
| $\sum\Delta J_{HH}$ MD/NMR (pH 11) | | | | 4.7 | 4.8 | 5.0 | 6.7 | 5.0 | 4.0 |
| $^3J_{CH}$ | *a* | | *a* | | | | | | |
| 3a-H, 1-C | | 1.4 | | 2.7 | 2.8 | 4.1 | 3.7 | 3.9 | 3.8 |
| 3a-H, 5-C | | <2 | | 2.3 | 2.0 | 2.1 | 2.4 | 2.5 | 2.2 |
| 3b-H, 1-C | | 5.2 | | 4.6 | 3.4 | 3.3 | 3.7 | 3.8 | 3.5 |
| 3b-H, 5-C | | <2 | | 2.3 | 1.9 | 2.9 | 3.0 | 2.4 | 2.0 |
| $\sum\Delta J_{CH}$ MD/NMR (pH 7) | | | | 2.5 | 3.1 | 5.6 | 5.2 | 4.8 | 4.3 |

[a] Heteronuclear ($^{13}$C−$^1$H) coupling constants in acidic and basic solution are difficult to measure. [b] Protocol 2: 22% Aa + 10% Ba + 1% Bb + 11 % Bc + 52% Ca + 1 %Cb + 3% Cc. For each *i*th conformational microstate, the average coupling constant can be computed from $^3J(HH) = \sum P_i{}^3J_i$ (HH); $^3J(HC) = \sum P_i{}^3J_i$ (HC); [$J_{3a,4a}$ = 22% × $J_{3a,4a}$ (Aa) + 10% × $J_{3a,4a}$ (Ba) + 1% × $J_{3a,4a}$ (Bb) + 11% × $J_{3a,4a}$ (Bc) + 52% × $J_{3a,4a}$ (Ca) + 1% × $J_{3a,4a}$ (Cb) + 3% × $J_{3a,4a}$ (Cc) = 10.4 Hz ($J_{obs}$ = 10.0)]. [c] Protocol 2: 44% Aa + 1% Ac + 21% Ba + 1% Bb + 33% Ca. [d] Protocol 4: 21% Aa + 1% Ac + 34% Ba + 11% Bb + 21% Ca + 12% Cb. [e] Protocol 4 (8 ps equilibration time): 20% Aa + 2% Ab + 34% Ba + 9% Ca + 22% Cb + 13% Cc. [f] Protocol 5: 9% Aa + 4% Ab + 40% Ba + 3% Bb + 3% Bc + 30% Ca + 1% Cb + 10% Cc. [g] Protocol 6: 22% Aa + 42% Ba + 31% Ca +5% Cc.

Bc) in agreement with the NMR data.

$$J_{3R,4S} = 22\% \times J_{3R,4S}\,(\mathrm{Aa}) + 10\% \times J_{3R,4S}\,(\mathrm{Ba}) + 11\% \times J_{3R,4S}\,(\mathrm{Bc}) + 52\% \times J_{3R,4S}\,(\mathrm{Ca}) = 10.4\ \mathrm{Hz}\ (J_{obs} = 10.0)$$

$$J_{3S,4R} = 22\% \times J_{3S,4R}\,(\mathrm{Aa}) + 10\% \times J_{3S,4R}\,(\mathrm{Ba}) + 11\% \times J_{3S,4R}\,(\mathrm{Bc}) + 52\% \times J_{3S,4R}\,(\mathrm{Ca}) = 10.5\ \mathrm{Hz}\ (J_{obs} = 10.3)$$

$$\sum J_{calc} - \sum J_{exp(3R,4S;3S,4R;3R,4R;3S,4S)} = 6.1\ \mathrm{Hz}$$

The fit between MD data and the experimental ones would also indicate that the conformational space was well sampled.[47,48] The small difference is attributed to a slight variation of the minor conformers that affects the conformational averaging in solution.

From the various averaging resulting from the MD approach, one set presented best minimized intramolecular energy and good agreement with the populations of rotamers obtained from NMR spectra (Table 7, Figure 8). The protocol with the presence of water molecules (protocol 6) or $\epsilon$ = 70 (protocol 4) from **22M**, or with $\epsilon$ = 5 from **21M** (protocol 2), seem to be generally the appropriate experi-

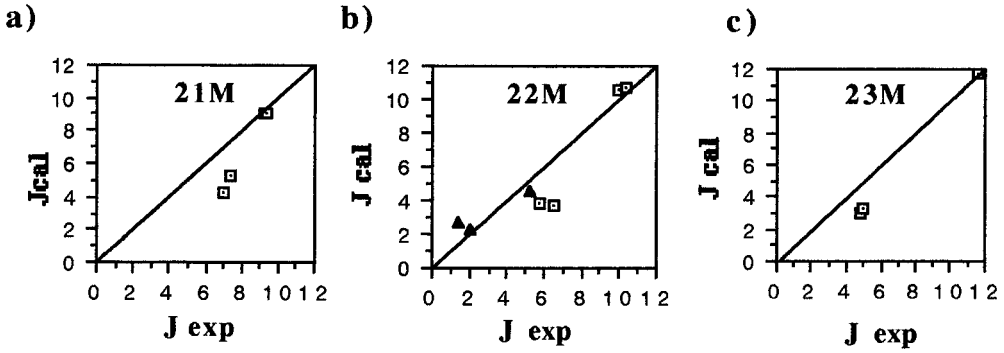


**Figure 8.** Correlation between the experimental (NMR) and calculated (MD) coupling constant using the MD runs that present the best correspondence in the population of rotamers between MD and NMR data for the different pH: (a) for **21M** solution, 21% Aa, 34% Ba, 21% Ca, 12% Cb, 11% Bb; (b) for **22M** solution, 22% Aa, 10% Ba, 52% Ca, 11% Bc and (c) for **23M** solution, 22% Aa, 42% Ba, 31% Ca. Key: ⊡, $J_{HH}$; ▲, $J_{CH}$.

ments since good agreement is observed with the NMR results.

In a box filled with water molecules (Table S2 of the Supporting Information, protocols 5 and 6) the compositions of the solutions correspond to 9% Aa + 40% Ba + 30% Ca + 10% Cc. The minor conformer Cc (10%) is generated with this protocol. In all the dynamics experiments considered, the *t*-**A**, $g^+$-**B**, and $g^-$-**C** conformers are stable and the energy of the *t*-**a** conformer is lower, confirming the results of NMR experiments (Table 2). At 300 K, no interconversion has been observed for Ca, and during only 800 ps, the Ca molecule leads to 784 Ca structures and 16 Cb (Figure 7b). It seems that a high energetic barrier between the three conformers prevents the interconversion from taking place in solution for the **2M** isomer as Aa is generated from Aa and Ab; Ba from Ba, Bb, Bc, and Cc; and Ca from Ca, Cb, and Ac (Table S2 of the Supporting Information, simulations at 300 K during 200 ps in a water box).

At neutral pH, the agreement between experimental (Table 2) and calculated (Table 7) results is quite satisfactory for experiments using the dielectric constant values $\epsilon = 5$ from **21M** (protocol 2), $\epsilon = 70$ from **22M** with 4 or 8 ps of equilibration time (protocol 4) and experiments with the presence of water molecules (protocol 5). In the graphs of Figure 8, we can observe a good agreement between the experimental NMR and the MD results, vs the best protocol (52% Ca, 22% Aa, 11% Bc, 10% Ba).

The problem in using MD searching for ligand binding conformations, particularly if the ligands are ions or highly charged molecules, is to not neglect protonation sites that will induce particular conformations. Thus, we have extended this study to different pH values. At pH 3 and 11, the electrostatic interactions are sufficiently reduced and several conformations are sterically favored for **21M** and **23M** (Table 6, protocols 1−4) according to the NMR results. The percentage of the **b** and **c** rotamers is important in **21M** (Table 6, protocol 4 with 8 ps of equilibration time, 20% Aa + 34% Ba + 9% Ca + 22% Cb + 13% Cc), and this is consistent with the NMR results (Table 2). At alkaline pH (Table 6, protocols 1 and 2), the preferred conformation of an unprotonated molecule is the sterically favored one, **a**. The percentage of the **a** rotamer is important (Table 6, from **23M**, protocol 2, 44% Aa + 21% Ba + 33% Ca or from **22M** in a water box, protocol 6, 22% Aa + 42% Ba + 31% Ca) and the two carboxylate groups are lying "extended", in agreement with the experimental NMR data (Table 2). A quantitative interpretation of these data shows that besides

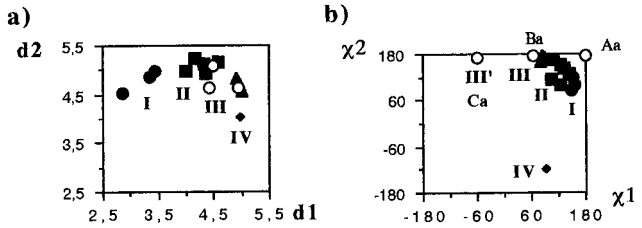


**Figure 9.** Identification of conformational families **I**−**IV** from the NMR and MD data of the cyclic isomers analogues (*cis*- and *trans*-C5 and *cis*- and *trans*-C6) and **2M**. They are represented in a diagram according to (a) their characteristic distances $d_{1(\alpha\text{-}NH_3^+ - \gamma\text{-}CO_2^-)}$ and $d_{2(\alpha\text{-}CO_2^- - \gamma\text{-}CO_2^-)}$ and (b) their characteristic torsion angles $\chi 1$ [$\alpha$-$CO_2^-$−C(2)−C(3)−C(4)] and $\chi 2$ [$^+$NC(2)−C(3)−C(4)−$\gamma CO_2^-$]. Key: ● **I**; ■, **II**; ▲, **III**; ◆, **IV**; ○, **2M**.

a minor electrostatic term $\alpha$-$NH_3^+$/$\gamma$-$CO_2^-$, a major steric repulsion exists in this analogue for such pairs of substituents as $\alpha$-Me/$\gamma$-$CO_2^-$ and $\alpha$-$CO_2^-$/$\gamma$-$CO_2^-$.

**Structural Characteristics of These Ligands.** We have compared the **2M** structures in terms of torsion angles $\chi 1$ [$\alpha$-CO−C(1)−C(2)−C(3)] and $\chi 2$ [C(1)−C(2)−C(3)-$\gamma$-$CO_2^-$] (Figure 9b and Table S3 of Supporting Information) corresponding to their relative flexibilities.

Rather than classify the conformational populations by combinations of $\chi 1$ and $\chi 2$, they have been collected according to the distance ($d_1$) and ($d_2$) (Figure 9a and Table S3 of Supporting Information). Two groups are considered in electrostatic interaction if their distance is less than (or equal to) 4 Å. In order to keep a limited number of classes **S** (**I**−**IV**), two distances were taken into account: $d_1$ ($\alpha$-NH−$\gamma$-$CO_2^-$) and $d_2$ ($\alpha$-CO−$\gamma$-$CO_2^-$). Two families were characterized by a $d_1$ distance shorter than $d_2$: **I** ($d_1 \ll d_2$) and **II** ($d_1 < d_2$). Conversely, two other families were characterized by a $d_2$ distance shorter than $d_1$: **III** ($d_2 < d_1$) and **IV** ($d_2 \ll d_1$). These four families (**I**−**IV**) are essentially characterized by the above-mentioned values of the two interatomic distances (Å) $d_1$ and $d_2$, but four other families **S′** (**I′**-**IV′**) with the same $d_1$ and $d_2$ distances will differ in the alkyl chain torsion angles $\chi 1$ and $\chi 2$.

The families **I**−**IV** corresponding to the different conformations, Ab (**I**), Aa (**II**), Ba (**III**), and Bc (**IV**), with these characteristics represent almost 60% of the **2M** solution, and in the same order, the families **I′**-**IV′** corresponding to the different conformations Ac, Cc (**I′**), Ca (**III′**), and Cb (**IV′**) with these characteristics are populated to ∼40% in **2M** solution, whatever the pH is.

The molecular modeling calculations on the **2M** isomers indicate that in the most stable conformations torsion angles

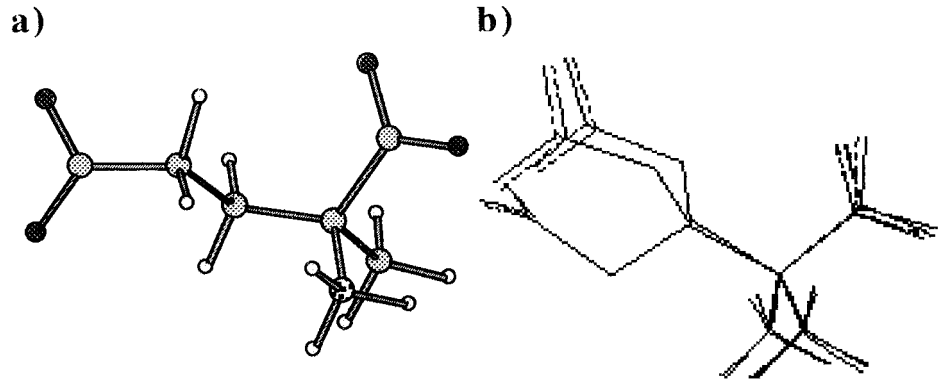


**Figure 10.** (a) Major conformation for **2M** at neutral pH generated by MD and in good agreement with NMR data, Ca; (b) superimposition of the major structures of **2M** at neutral pH (Ca, Ba, and Aa). Hydrogens have been removed for clarity on the backbones except on methyl, α-$NH_3^+$, and γ-$CO_2H$.,

χ1 are of ∼±60° and χ2 of ∼180°. The calculations have included the hydration effects of the aqueous solvent. This corresponds to the most populated conformations of **2M** in NMR solution. The conformations $g^-t$-Ca and $g^+t$-Ba are 60% populated, the very extended conformation *tt*-Aa representing ∼20% of the **2M** solution. The folded conformations $g^+g^-$-Bc and $g^-g^-$-Cc are 10% populated, being unfavorable.

The superimposition of C(1) and of the central atoms of the two functional groups, i.e., the α-N and C(2) (α-CO) of the different conformers (Aa, Ba, Ca), deduced from NMR and MD data of the **2M** analogue, presents several conformational similarities (Figure 10).

**Comparison with Other Active Glutamate Analogues, Substituted on the C(2) Carbon.** The 2-methylglutamate, substituted by a methyl at the C(2) carbon, can be compared to the two cyclic compounds (Figure 1) substituted at the same carbon (C5, C6) according to the major conformations existing in solution and to their biological activities (Figure 9).

In all the compounds, the ring closure does not allow a negative gauche $g^-$ value for the two torsion angles (χ1 and χ2), like $g^-$-**C** and $g^-$-**c**. The *cis*-C5-ACPD belongs to the families **II** (Aa), **III** (Ba), and **IV** (Bc) while the families **I** (Ab), **II** (Aa), and **III** (Ba) represent the *trans*-C5-ACPD. The preferred conformational classes of the *cis*- and *trans*-C6 molecule are limited to the **II** (Aa) and **IV** (Bc) families and the **I** (Ab) and **III** (Ba) families, respectively. This study showed that the conformer $g^-t$-Ca is the major one of 2-methylglutamic acid. This conformation is totally forbidden in all the cyclic compounds.

Our previous studies on cyclic C5 and C6[19,20] and on β- and γ-methylated glutamic acid analogues[21] have shown that the major conformation in solution of specific agonists is $tg^-$-Ac relative to the ionotropic KA receptor, $tg^+$-Ab relative to the metabotropic mGluR1a receptor, and $g^+g^-$-Bc conformation relative to the ionotropic NMDA receptor. When the glutamic acid residue was α-methylated, only the conformation $g^-t$-Ca was involved and, the 2-methylglutamic acid was totally inactive.

## CONCLUSION

From these results, it can be concluded that the presence of the methyl in a particular position on the linear alkyl chain led to a restricted number of conformations. An extensive conformational study has clearly established the privileged conformation of this analogue. It is to be noted that the major solution conformation of 2-methylglutamate (inactive molecule) does not present the same structural analogy compared to the structure of the specific inducers of the glutamate receptor. Thus, it seems difficult to reach a particular high free-energy conformation adopted by the molecule after binding to the receptor, if the different groups potentially active in the binding site (α-$COO^-$, α-$NH3^+$, γ-$COO^-$) do not present beforehand a particular spatial topology.

## MATERIALS AND METHODS

**(a) NMR Experiments.** 2-Methylglutamic acid was purchased from Aldrich Chemicals and used without further purification. The compound were dissolved in deuterium oxide in a $NaD_2PO_4-Na_2DPO_4$ buffer (0.5 M) and at a concentration of 0.06 mol $dm^{-3}$ at pH 7. All chemical shifts are expressed in ppm downfield from TMS. All NMR experiments were carried out on a Bruker AMX 500 spectrometer. The proton spectra were recorded at different temperatures from 7 to 37 °C with a 10 °C step size (Table S1 of the Supporting Information). The accuracy of the temperature was found to be ±0.1 °C. The spectrum simulation was done on a Macintosh II computer using software NMR II. Presaturation of the solvent with two decoupling powers was used for all 1D and 2D experiments. The distortionless enhancement by polarization transfer (DEPT) polarization transfer from $^1H$ to $^{13}C$ nuclei (with $^1H$ BB decoupling) spectra was acquired and tuned for optimum polarization transfer with $^1J_{CH}$ of 135 Hz.

The 2D $^1H-^1H$ COSY spectra were acquired by recording 256 FIDs of 1024 points. The relaxation delay was set to 4.0 s. The spectral width was set to 2500 Hz for proton spectra and 31 250 Hz for carbon spectra. The 90° pulse was 8.0 μs, the relaxation delay was 4.0 s, and each FID was acquired with 64 scans. 2D spectral processing was performed on an X32 computer using UXNMR software (Bruker). The data were zero-filled, and the final size of the matrices was 2K × 1K to 1024 and 1024 points in $f_2$ and $f_1$, respectively, prior to double Fourier transformations with an unshifted sine-bell window function in both dimensions.

The inverse correlation $^1H-^{13}C$ and $^1H-^{15}N$ HMBC experiments [pulse field gradient-heteronuclear multiple-bond correlation (PFG-HMBC)] were recorded at 300 K using a transfer delay of 80 ($^{13}C$) or 50 ms ($^{15}N$), with 256

experiments of 1024 data points, a sweep width of 3876 Hz in $f_2$ and 26 412 ($^{13}$C) or 20 275 Hz ($^{15}$N) in $f_1$. One millisecond half-sinusoid gradients of 20, 20, and 10 ($^{13}$C) or 20, 10, and 6.95 G cm$^{-1}$ ($^{15}$N) were used to select protons attached to carbon and the delay of 80 ($^{13}$C) or 50 ms ($^{15}$N) which was optimum for two- or three-bond couplings (delay $^1/_2\ ^3J_{XH}$ delay). The 90° nonselective proton pulses were 9.5 $\mu$s long while the 90° nonselective carbon or azote was 10.5 or 20 $\mu$s, respectively. A low-pass $J$ filter was used with a value of 3.5 ms for the $\Delta = {}^1/_2\ J_{CH}$ delay optimum to keep $^1J_{CH}$ connectivity.

Long-range $^{13}$C−$^1$H coupling constant by 2D $J-\delta$ selective INEPT experiment was carried out in the solution of **2M** (Table 2). The selectivity was achieved by a DANTE-type pulse train generated by the decoupler channel. The selectivity was equal to $\delta$ $^1$H ± 50 Hz ($\gamma\ B_1{}^2\pi = 50$ Hz). The 90° nonselective proton pulses were 45 $\mu$s long. A value of 45 ms for the $\Delta$ delay was optimum for $J$ coupling of 5 Hz. The relaxation delay was 6 s, and each FID was acquired with 256 scans with broad-band decoupling. Experiments were achieved, and data were zero-filled to 512 points in the $f_1$ dimension. In the $f_2$ dimension, data were acquired with 4096 points, and no zero-filling was applied before Fourier transformation. The final resolutions were 0.1 and 7.0 Hz per points in the $f_1$ ($J_{C,H}$) and $f_2$ ($^{13}$C chemical shifts) dimensions, respectively. Resolution enhancement by Gaussian transformation was realized both in $f_2$ and $f_1$ dimensions. The $t_{1/2}$ was initially set to a value of 3 $\mu$s and was incremented by 8 ms per experiment.

**(b) Molecular Dynamics and Molecular Mechanics Calculations.** Computer modeling was carried out with BIOSYM molecular modeling software on a Silicon Graphics workstation. Initial calculations started with coordinates for the nine structures built using the Insight II builder module with dielectric constants between 1 and 78 (Table 4). Considering the NMR data a distance-dependent dielectric, $\epsilon = R_{ij}$ or $\epsilon = 4R_{ij}$, was not correct as it did not allow us to confirm the result obtained by NMR spectroscopy. A second protocol, to mimic the solvent effect, can be used with explicit solvent molecules incorporated during the run. The atoms of the system that is to be simulated are put into a cubic (12-12-12 Å)-shaped box surrounded by identical translated images of itself (PBC). Only interactions with nearest neighbors are taken into account. The anisotropy of the interaction due to the cubic shape of the nearest image box can be avoided by the application of a spherical cutoff (radius $R_c$). About 48 water molecules are needed to fill the remaining empty space (after insertion of the solute) in the box. The periodic boundary conditions assume that when an atom leaves the central box on one side, it enters it with identical velocity at the opposite side at the translated image position. The relative permittivity was set to $\epsilon = 1$ and the energies obtained are those of "molecule + 48$H_2O$" systems. Thus, the energies of the corresponding minimized molecules were very difficult to evaluate, as well as their relative populations. Molecular dynamics simulations with different starting structures were carried out using a step size of 1 fs at 500 K for 50 ps. The molecular dynamics simulations were initiated following standard methods, and the system was allowed to come to equilibrium for 8 ps. The temperature was then reduced to 300 K and the simulation continued for 200 ps. Molecular dynamics at 500 and 300 K for a total of 100 ps were calculated with a time step of 1 fs, and structures were sampled every 1 ps. Sampling every picosecond was used for the analysis, and structures with the lowest energy were selected as relevant conformations.

## ACKNOWLEDGMENT

We thank J. Hart-Davis for skillful assistance.

**Supporting Information Available:** Tables of coupling constants simulations of the conformations, and physical features and a figure of NMR spectra at varying temperatures (4 pages). Ordering information is given on any current masthead page.

## REFERENCES AND NOTES

(1) Watkins, J. C.; Krogsgaard-Larsen, P.; Honoré, T. Structure−activity relationships in the development of excitatory amino acids receptors. *Trends Pharmacol. Sci.* **1990**, *11*, 25−33.
(2) Chamberlin, R.; Bridges, R. In *Conformationally constrained acidic amino acids as probes of Glutamate receptors and transporters*; Kozikowski, A., Ed.; Raven Press: New York, 1993; Chapter 9, pp 231−259.
(3) Pratviel-Sosa, F.; Acher, F.; Trigalo, F.; Blanot, D.; Azerad, R.; van Heijenoort, J. Effect of various analogues of D-glutamic acid on the d-glutamate-adding enzyme from *Escherichia coli*. *FEMS Microbiol. Lett.* **1994**, *115*, 223−228.
(4) Gass, J. D.; Meister, A. Computer analysis of the active site of glutamine synthetase. *Biochemistry* **1970**, *9*, 1380−1389.
(5) Monoghan, D. T.; Bridges, R. J.; Cotman, C. W. The excitatory amino acid receptors: their classes, pharmacology and distinct properties in the function of the central nervous system. *Annu. Rev. Pharmacol. Toxicol.* **1989**, *29*, 365.
(6) Bliss, T. V. P.; Collingridge, G. L. A synaptic model of memory: long term potentiation in the hyppocampus. *Nature* **1993**, *361*, 31−39.
(7) Choi, D. W. Glutamate neurotoxicity and diseases of the nervous system. *Neuron* **1988**, *1*, 623−643.
(8) Meldrum, B.; Garthwaite, J. Excitatory amino acid neurotoxicity and neurodegenerative disease. *Trends Pharmacol. Sci.* **1990**, *11*, 379−387.
(9) Nakanishi, S. Molecular diversity of glutamate receptors and implications for brain function. *Science* **1992**, *258*, 597−603.
(10) Pin, J. P.; Duvoisin, R. The metabotropic glutamate receptors: Structure and functions. *Neuropharmacology* **1995**, *34*, 1−26.
(11) Schoepp, D. D.; Conn, P. J. Metabotropic glutamate receptors in brain function and pathology. *Trends Pharmacol. Sci.* **1993**, *14*, 13−20.
(12) Stratton, K. R.; Worley, P. F.; Baraban, J. M. Excitation of hyppocampal neurons by stimulation of glutamate Qp receptors. *Eur. J. Pharmacol.* **1989**, *173*, 235−237.
(13) Pin, J. P.; Bockaert, J. *Curr. Opin. Neurobiol.* **1995**, 342−349.
(14) Conquet, F.; Bashir, Z. I.; Davies, C. H.; Daniel, H.; Ferraguti, F.; Bordi, F.; Franz-Bacon, K.; Reggiani, A.; Matarese, V.; Condé, F.; Colingridge, G. L.; Crépel, F. Motor deficit and impairment of synaptic plasticity in mice lacking mGluR1. *Nature* **1994**, *372*, 237−243.
(15) Curry, K.; Peet, M. J.; Magnuson, D. S. K.; McLennan, H. Synthesis, resolution, and absolute configuration of the isomers of the neuronal excitant1-amino-1,3-cyclopentanedicarboxylic acid. *J. Med. Chem.* **1988**, *31*, 864−867.
(16) Kozikowski, A. P.; Fauq, A. H. Probing the topography of Kainate recognition sites: Synthesis of a novel oxetane containing kainic acid analogue. *Tetrahedron Lett.* **1990**, *31*, 2967.
(17) James, V. A.; Walker, R. J.; Wheal, H. V. Structure−activity studies on an excitatory receptor for glutamate on leech retzius neurones. *Br. J. Pharmacol.* **1980**, *68*, 711−717.
(18) Palmer, E.; Monoghan, D. T.; Cotman, C. W. Trans-ACPD, a selective agonist of phosphoinositide-coupled excitatory amino acid receptors. *Eur. J. Pharmacol.* **1989**, *166*, 585−587.
(19) Morelle, N.; Gharbi-Benarous, J.; Acher, F.; Valle, G.; Crisma, M.; Toniolo, C.; Azerad, R.; Girault, J. P. Conformational analysis of cyclohexane-derived analogues of glutamic acid by X-ray crystallography, NMR spectroscopy in solution and molecular dynamics. *J. Chem. Soc., Perkin Trans. 2* **1993**, 525−533.
(20) Larue, V.; Gharbi-Benarous, J.; Acher, F.; Valle, G.; Crisma, M.; Toniolo, C.; Azerad, R.; Girault, J. P. Conformational analysis by NMR spectroscopy, molecular dynamics simulation in water and X-ray crystallography of glutamic acid analogues: Isomers of 1-amino -1,3 cyclopentane dicarboxylic acid (ACPD). *J. Chem. Soc., Perkin Trans. 2* **1995**, 1111−1126.
(21) Todeschi, N.; Gharbi-Benarous, J.; Acher, F.; Azerad, R.; Girault, J. P. Conformational analysis by NMR spectroscopy and molecular

simulation in water of methylated glutamic acids, agonists at glutamate receptors. *J. Chem. Soc., Perkin Trans. 2* **1996**, 1337−1351.
(22) Gu, Z. Q.; Hesson, D.; Pelletier, J. C.; Meccecchini, M. L. Synthesis, resolution and biological evaluation of the four stereoisomers of 4-methylglutamic acid: Selective probes of kainate receptors. *J. Med. Chem.* **1995**, *38*, 2518−2520.
(23) Pin, J. P.; Bockaert, J., unpublished results, 1996.
(24) Altmann, K. H.; Altmann, E.; Mutter, M. Conformational study on peptides containing enantiomeric α-methyl α-amino acids. *Helv. Chim. Acta* **1992**, *75*, 1198−1210.
(25) Paterson, Y.; Ramsey, S. M.; Benedetti, E.; Nemethy, G.; Scheraga, H. A. Sensitivity of polypeptide conformation to geometry. Theoretical conformational analysis of oligomers of α-aminoisobutyric acid. *J. Am. Chem. Soc.* **1981**, *103*, 2947−2955.
(26) Valle, G.; Crisma, M.; Toniolo, C.; Beisswenger, R.; Rieker, A.; Jung, C. First observation of a helical peptide containing a chiral residue without a preferred screw sense. *J. Am. Chem. Soc.* **1989**, *111*, 6828.
(27) Pavone, V.; DiBlasio, B. A.; Santini, A.; Benedetti, E.; Pedone, C.; Toniolo, C.; Crisma, M. The longest regular polypeptide 3(10) helix at atomic resolution. *J. Mol. Biol.* **1990**, *214*, 633.
(28) Altona, C.; Sundaralingam, M. Conformational analysis of the sugar ring in nucleosides and nucleotides. Improved metodes for the interpretation of proton magnetic resonance coupling constants. *J. Am. Chem. Soc.* **1973**, *95*, 2333−2344.
(29) Haasnoot, C. A. G.; De Leeuw, F. A. A. M.; Altona, C. The relation between proton−proton NMR coupling constants and substituent electronegativities. I. An empirical generalization of the Karplus equation. *Tetrahedron* **1980**, *36*, 2783−2792.
(30) Tvaroska, I.; Hricovini, M.; Petrakova, E. An attemp to derive a new Karplus-type equation of vicinal proton−carbon coupling constants for C-O-C-H segments of bonded atoms. *Carbohydr. Res.* **1989**, *189*, 359−362.
(31) De Marco, A.; Llinas, M.; Wüthrich, K. Analysis of the $^1$H-NMR spectra of ferrichrome peptides. II. The amide resonances. *Biopolymers* **1978**, *17*, 637−650.
(32) Bendall, M. R.; Pegg, D. T. Complete accurate editing of decoupled carbon-13 spectra using DEPT and a quaternary-only sequence. *J. Magn. Reson.* **1983**, *53*, 272−296.
(33) Bax, A. Structure determination and spectral assignment by pulsed polarization transfer via long-range $^1$H−$^{13}$C couplings. *J. Magn. Reson.* **1984**, *57*, 314−318.
(34) Lin, L. J.; Cordell, G. A. Application of the SINEPT pulse programme in the structure elucidation of coumarinolignans. *J. Chem. Soc., Chem. Commun.* **1986**, 377−379.
(35) Hurd, R. E.; John, B. K. Gradient-enhancement proton-detected heteronuclear multiple-quantum coherence spectroscopy. *J. Magn. Reson.* **1991**, *91*, 648−653.
(36) Kessler, H.; Griesinger, C.; Wagner, K. Peptide conformation. 42. Conformation of side chains in peptides using heteronuclear coupling constants obtained by two-dimensional NMR spectroscopy. *J. Am. Chem. Soc.* **1987**, *109*, 6927.
(37) Ladam, P.; Gharbi-Benarous, J.; Pioto, M.; Delaforge, M.; Girault, J. P. Determination of long-range $^{13}$C−$^1$H coupling constants of macrolide antibiotics by 2D J-$\delta$ selective INEPT experiments. *Magn. Reson. Chem.* **1994**, *32*, 1−7.
(38) Roberts, G. C. K.; Jardetzky, O. Nuclear magnetic resonance spectroscopy of amino acids, peptides, and proteins. *Adv. Protein Chem.* **1970**, *24*, 447−545.
(39) Jardetzky, O.; Roberts, G. C. K. *NMR in Molecular Biology*; Academic Press: New York, 1981.
(40) Jardetzky, O. On the nature of molecular conformations inferred from high-resolution NMR. *Biochim. Biophys. Acta* **1980**, *621*, 227−232.
(41) De Marco, A.; Llinas, M.; Wüthrich, K. $^1$H−$^{15}$N Spin−Spin Couplings in Alumichrone. *Biopolymers* **1978**, *17*, 2727−2742.
(42) De Marco, A.; Llinas, M. *Biochemistry*. **1979**, *18*, 3846.
(43) Dauber-Osguthorpe, P.; Roberts, V. A.; Osguthorpe, D. J.; Wolff, J.; Genest, M.; Hagler, A. T. Structure and energetics of ligand binding to proteins: E. coli dihydrofolate reductase-trimethoprim, A drug-receptor system. *Proteins: Struct., Funct. Genet.* **1988**, *4*, 31−47.
(44) Burt, S. K.; Mackay, D.; Nagler, A. T. In *Computer-Aided Drug Design*; Perun, T. J., Propst, C. L., Eds.; Marcel Dekker: New York, 1989; p 66.
(45) van Gunsteren, W. F.; Berendsen, H. J. C. Computer Simulation of molecular dynamics: methodology, applications, and perspectives in chemistry. *Angew. Chem., Int. Ed. Engl.* **1990**, *29*, 992−1023.
(46) Weiner, S. J.; Kollmann, P. A.; Case, D. C.; Singh, U. C.; Ghio, C.; Alagona, G.; Profeta, S.; Weiner, P. A new force field molecular mechanical simulation of nucleic acids and proteins. *J. Am. Chem. Soc.* **1984**, *106*, 765−784.
(47) Kessler, C.; Griesinger, C.; Lautz, J.; Müller, A.; van Gunsteren, W. F.; Berendsen, H. J. C. Conformational dynamics detected by nuclear magnetic resonance NOE values and *J* coupling constants. *J. Am. Chem. Soc.* **1988**, *110*, 3393−3396.
(48) Hünenberger, P. H.; Mark, A. E.; van Gunsteren, W. F. *J. Mol. Biol.* **1995**, *252*, 492−503.

CI9600521